Journal of Sound and Vibration (1999) **225**(5), 915–934
Article No. jsvi.1999.2262, available online at http://www.idealibrary.com on IDEAL®

ANALYSIS OF VIBRATING THICK RECTANGULAR PLATES WITH MIXED BOUNDARY CONSTRAINTS USING DIFFERENTIAL QUADRATURE ELEMENT METHOD

F.-L. LIU

CAD/CAM Laboratory, Division of Engineering Mechanics, School of Mechanical and Production Engineering, Nanyang Technological University, Singapore 639798, *Singapore*

AND

K. M. LIEW

Center for Advanced Numerical Engineering Simulations, School of Mechanical and Production Engineering, Nanyang Technological University, Singapore 639798, *Singapore*

(*Received* 30 *November* 1998, *and in final form* 17 *March* 1999)

A free vibration analysis of moderately thick rectangular plates with mixed boundary conditions is presented on the basis of the first-order shear deformation plate theory. The differential quadrature element method, a highly efficient and accurate hybrid approach, has been employed. To establish the numerical model, the complex plate domain is first decomposed into small simple continuous sub-domains (elements) and the differential quadrature method is then applied to each continuous sub-domain to solve the problems. Compatibility conditions are developed for the conjunction nodes on the interface boundaries of elements in order to connect the elements. Convergence and comparison studies are carried out to establish the reliability of the solutions. The first eight frequency parameters are predicted for various types of thick rectangular plates with mixed edge constraints.

1. INTRODUCTION

Problems of rectangular plates with mixed edge constraints have been investigated by many researchers adapting different solution techniques. Ota and Hamada [1] predicted the fundamental frequencies of a simply supported rectangular plate partially clamped on the edge using a distributed moment function along the mixed edge. Keer and Stahl [2] studied the same problem by means of Fredholm integral equations of a second kind, and demonstrated the dependence of the fundamental frequencies on the clamped portion. Narita [3] employed a series-type solution approach to solve the problem and obtained the frequency parameters for wide ranges of mixed-edge rectangular plates. Other numerical methods such as the finite element method [4], superposition method [5], spline finite strip method [6], spline element method [7], and the Rayleigh–Ritz method [8–10] have also been used to study the free vibration of rectangular plates with discontinuous edge

0022-460X/99/350915 + 20 $30.00/0

constraints. Laura and Gutierrez tried to predict the fundamental frequency of the simply supported rectangular plates partially clamped along one and two edges by using the global differential quadrature method [11]. However, all the research work mentioned above is all confined to thin plates, solutions to thick rectangular plates with discontinuous boundary constraints are scarce in the literature. Only one paper was found to have treated the problem of free vibration of the Mindlin plate with mixed boundary constraints [12], but only the fundamental frequencies of the thin plates for two simple cases were calculated. The primary purpose of this paper is to solve the free vibration problems of thick rectangular plates with mixed boundary constraints. A hybrid approach namely the differential quadrature element method, which combines the differential quadrature method with the domain decomposition method, has been employed.

The differential quadrature (DQ) method originated with Bellman and his associates [13] and was first applied to the structural analysis field by Bert and his associates [14–16]. Since then, many studies researches have been done in both the theoretical development and the engineering applications of the method. In all of the applications, this method yielded good to excellent results for only a few discrete points due to the use of the high-order global-based functions in the computational domain. An excellent review paper contributed by Bert and Malik [17] has summarized a detailed literature list on both aspects of the DQ method. Nevertheless, further application of the method has been greatly restricted by its drawback of not being able to be directly employed to solve the problem with discontinuities. To overcome such a drawback, the DQ method has been combined with the domain decomposition method first by Striz *et al.* [18–20] and then by Wang and Gu [21, 22] to solve the static problems of truss and beams and the static and free vibration problems of thin plates. This hybrid approach has been further developed by Han and Liew to solve the one-dimensional bending problem of the axisymmetric shear deformable circular plate [23], and by the present author to solve two-dimensional bending and vibration problems of thick rectangular plates and polar plates having discontinuities [24–28]. In this study, the differential quadrature method is combined with the domain decomposition method to deal with the free vibration problems of the moderately thick rectangular plates with mixed boundary constraints.

2. MATHEMATICAL FORMULATIONS

Consider a moderately thick rectangular plate with side lengths $a \times b$ as shown in Figure 1. The plate is divided into N_E elements based on the discontinuities in the geometry, boundary constraints and materials used. Each element consists of an isotropic material and has uniform thickness and continuous boundary constraints on each edge.

2.1. EIGENVALUE EQUATION AND BOUNDARY CONSTRAINT CONDITIONS

For a given element l of the plate, the eigenvalue equations for the free vibration problems can be written based on the first order shear deformation theory as

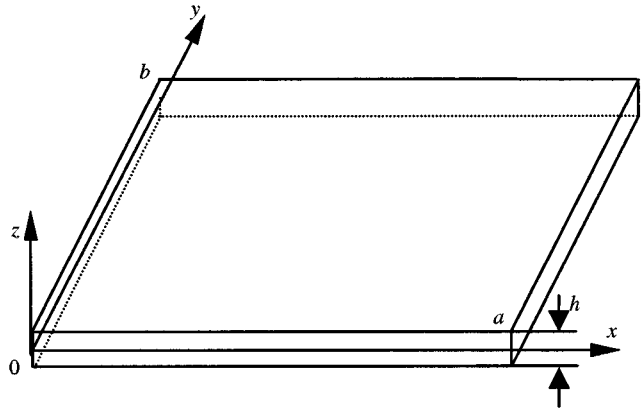

Figure 1. Configuration of a thick rectangular plate.

follows [29]:

$$\frac{\partial^2\psi_x}{\partial x^2}+\frac{(1-\nu_l)}{2}\frac{\partial^2\psi_x}{\partial y^2}+\frac{(1+\nu_l)}{2}\frac{\partial^2\psi_y}{\partial x\partial y}-\frac{\kappa G_l h_l}{D_l}\left(\frac{\partial w}{\partial x}+\psi_x\right)=\frac{\rho_l h_l^3}{12D_l}\frac{\partial^2\psi_x}{\partial t^2}, \quad (1)$$

$$\frac{(1+\nu_l)}{2}\frac{\partial^2\psi_x}{\partial x\partial y}+\frac{\partial^2\psi_y}{\partial y^2}+\frac{(1-\nu_l)}{2}\frac{\partial^2\psi_y}{\partial x^2}-\frac{\kappa G_l h_l}{D_l}\left(\frac{\partial w}{\partial y}+\psi_y\right)=\frac{\rho_l h_l^3}{12D_l}\frac{\partial^2\psi_x}{\partial t^2}, \quad (2)$$

$$\left(\frac{\partial^2 w}{\partial x^2}+\frac{\partial^2 w}{\partial y^2}\right)+\left(\frac{\partial\psi_x}{\partial x}+\frac{\partial\psi_y}{\partial y}\right)=\frac{\rho_l}{\kappa G_l}\frac{\partial^2 w}{\partial t^2}, \quad (3)$$

where w, ψ_x and ψ_y are the transverse deflection, the rotation of the normal about the y-axis and the rotation of the normal about the x-axis respectively: h_l, E_l, G_l and ν_l are the thickness of the plate, Young's modulus, shear modulus and Poisson's ratio, respectively; D_l is the plate flexural rigidity; and κ is the shear correction factor. For free vibration analysis, κ is taken to be $\pi^2/12$. Letting $w = W(x, y)e^{j\omega t}$, $\psi_x = \Psi_x(x, y)e^{j\omega t}$, $\psi_y = \Psi_y(x, y)e^{j\omega t}$ and $\omega = \Omega\sqrt{E/[\rho a^2(1-\nu^2)]}$ and substituting them into equations (1)–(3), one can obtain the following equations:

$$\frac{\partial^2\Psi_x}{\partial x^2}+\frac{(1-\nu_l)}{2}\frac{\partial^2\Psi_x}{\partial y^2}+\frac{(1+\nu_l)}{2}\frac{\partial^2\Psi_y}{\partial x\partial y}-F_l\left(\frac{\partial W}{\partial x}+\Psi_x\right)=-\Omega^2/a^2\Psi_x, \quad (4)$$

$$\frac{(1+\nu_l)}{2}\frac{\partial^2\Psi_x}{\partial x\partial y}+\frac{\partial^2\Psi_y}{\partial y^2}+\frac{(1-\nu_l)}{2}\frac{\partial^2\Psi_y}{\partial x^2}-F_l\left(\frac{\partial W}{\partial y}+\Psi_y\right)=-\Omega^2/a^2\Psi_y, \quad (5)$$

$$\left(\frac{\partial^2 W}{\partial x^2}+\frac{\partial^2 W}{\partial y^2}\right)+\left(\frac{\partial\Psi_x}{\partial x}+\frac{\partial\Psi_y}{\partial y}\right)=\frac{-2}{\kappa(1-\nu_l)a^2}\Omega^2 W \quad (6)$$

in which

$$F_l = 6\kappa(1 - \nu_l)/h_l^2. \tag{7}$$

The moments and shear forces are expressed as

$$M_x = D_l\left(\frac{\partial \psi_x}{\partial x} + \nu_l \frac{\partial \psi_y}{\partial y}\right), \tag{8a}$$

$$M_y = D_l\left(\nu_l \frac{\partial \psi_x}{\partial x} + \frac{\partial \psi_y}{\partial y}\right), \tag{8b}$$

$$M_{xy} = \frac{1 - \nu_l}{2} D_l\left(\frac{\partial \psi_x}{\partial y} + \frac{\partial \psi_y}{\partial x}\right), \tag{8c}$$

$$Q_x = \kappa G_l h_l\left(\frac{\partial w}{\partial x} + \psi_x\right), \quad Q_y = \kappa G_l h_l\left(\frac{\partial w}{\partial y} + \psi_y\right). \tag{9a,b}$$

The boundary conditions for the edge $x = 0$ can be expressed as follows.

Clamped edge (C):

$$w = 0, \quad \psi_x = 0, \quad \psi_y = 0. \tag{10}$$

Hard simply supported edge (S):

$$w = 0, \quad \psi_y = 0, \quad M_x = 0. \tag{11}$$

Soft simply supported edge (S′):

$$w = 0, \quad M_x = 0, \quad M_{xy} = 0. \tag{12}$$

Free edge (F):

$$Q_x = 0, \quad M_x = 0, \quad M_{xy} = 0. \tag{13}$$

2.2. RECTANGULAR FREE VIBRATION DQ PLATE ELEMENT

The lth element is further divided into $N_x \times N_y$ grid points in the x and y directions as shown in Figure 2. Using the DQ procedures [17], the discrete governing equations for free vibration of the lth plate element can be expressed at each discrete point of the inner mesh into

$$\sum_{k=1}^{N_{lx}} C_{ik}^{(2)}(\Psi_x)_{kj} + \frac{(1 - \nu_l)}{2} \sum_{m=1}^{N_{ly}} \bar{C}_{jm}^{(2)}(\Psi_x)_{im} - F_l(\Psi_x)_{ij}$$

$$+ \frac{(1 + \nu_l)}{2}\left[\sum_{k=1}^{N_{lx}} C_{ik}^{(1)} \sum_{m=1}^{N_{ly}} \bar{C}_{jm}^{(1)}(\Psi_y)_{km}\right] - F_l \sum_{k=1}^{N_{lx}} C_{ik}^{(1)}(W)_{kj} = -\Omega^2/a^2(\Psi_x)_{ij}, \tag{14a}$$

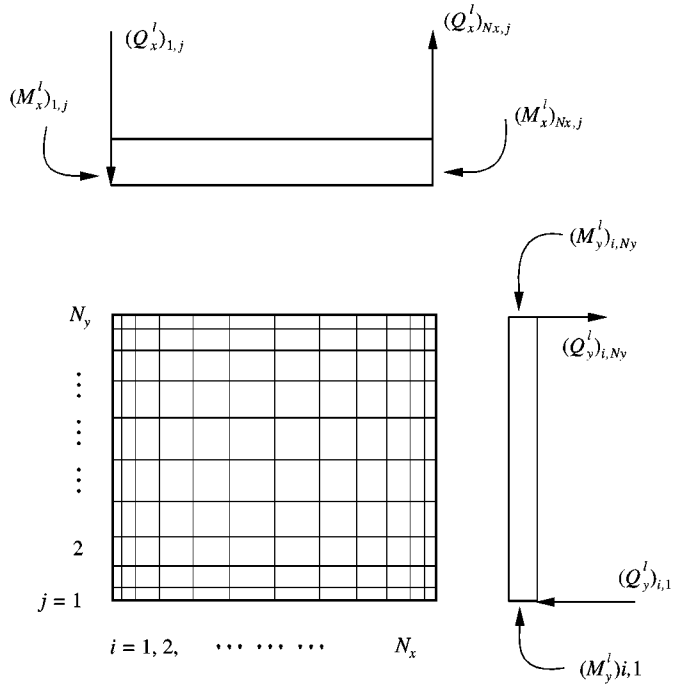

Figure 2. Arrangement of grid points for element l.

$$\frac{(1+\nu_l)}{2}\left[\sum_{k=1}^{N_{lx}} C_{ik}^{(1)} \sum_{m=1}^{N_{ly}} \bar{C}_{jm}^{(1)}(\Psi_x)_{km}\right] + \sum_{m=1}^{N_{ly}} \bar{C}_{jm}^{(2)}(\Psi_y)_{im}$$

$$+ \frac{(1+\nu_l)}{2} \sum_{k=1}^{N_{lx}} C_{ik}^{(2)}(\Psi_y)_{kj} - F_l(\Psi_y)_{ij} - F_l \sum_{m=1}^{N_{ly}} \bar{C}_{jm}^{(1)}(W)_{im} = -\Omega^2/a^2(\Psi_y)_{ij}, \tag{14b}$$

$$\sum_{k=1}^{N_{lx}} C_{ik}^{(2)}(W)_{kj} + \sum_{m=1}^{N_{ly}} \bar{C}_{jm}^{(2)}(W)_{im} + \sum_{k=1}^{N_{lx}} C_{ik}^{(2)}(\Psi_x)_{kj} + \sum_{m=1}^{N_{ly}} \bar{C}_{jm}^{(1)}(\Psi_y)_{im}$$

$$= \frac{-2}{\kappa(1-\nu_l)a^2}\Omega^2 W_{ij}, \quad i = 1, 2, 3, \ldots, N_x, \quad j = 1, 2, 3, \ldots, N_y$$
$$\text{and } l = 1, 2, 3, \ldots, N_E \tag{14c}$$

where $C_{rs}^{(n)}$ and $\bar{C}_{rs}^{(n)}$ $(r = 1, 2, 3, \ldots, N_x;\ s = 1, 2, 3, \ldots, N_y)$ are the weighting coefficients for the nth-order partial derivatives of w, ψ_x and ψ_y with respect to the global co-ordinates x and y.

Equations (14a–c) can be further expressed in matrix form as

$$\mathbf{K}^e\mathbf{d}^e = \lambda\mathbf{B}^e\mathbf{d}^e, \tag{15}$$

where $\lambda = (\rho h \omega^2 a^4/D)^{1/2}$ is defined as the frequency parameter: $\mathbf{K}^e$, $\mathbf{d}^e$ and $\mathbf{B}^e$ are the element weighting coefficient matrix, element displacement vector and the element consistent mass matrix, respectively. Also

$$\mathbf{d}^e = [w_{1,1}, \psi_{x1,1}, \psi_{y1,1}, w_{1,2}, \psi_{x1,2}, \psi_{y1,2}, \ldots, w_{N_x,N_y}, \psi_{xN_x,N_y}, \psi_{yN_x,N_y}]^{\mathrm{T}}, \quad (16)$$

$$\mathbf{B}^e = [\mathbf{b}^e_{1,1}, \mathbf{b}^e_{1,2}, \ldots, \mathbf{b}^e_{1,N_y}, \mathbf{b}^e_{2,1}, \mathbf{b}^e_{2,2}, \ldots, \mathbf{b}^e_{2,N_y}, \ldots, \mathbf{b}^e_{N_x,1}, \ldots, \mathbf{b}^e_{N_x,N_y}]^{\mathrm{T}}, \quad (17)$$

where $\mathbf{b}^e_{1,1}, \mathbf{b}^e_{1,2}, \ldots, \mathbf{b}^e_{1,N_y}, \mathbf{b}^e_{2,1}, \mathbf{b}^e_{2,2}, \ldots, \mathbf{b}^e_{2,N_y}, \ldots, \mathbf{b}^e_{N_x,1}, \mathbf{b}^e_{N_x,2}, \ldots, \mathbf{b}^e_{N_x,N_y}$ are null matrices with $3N \times 3$ elements, and $\mathbf{b}^e_{2,2}, \ldots, \mathbf{b}^e_{2,N_y-1}, \ldots, \mathbf{b}^e_{N_x-1,2}, \ldots,$ and $\mathbf{b}^e_{N_x-1,N_y-1}$ are matrices with $3N \times 3$ elements, in which only the three elements at the corresponding point in each matrix are not equal to zero; the other elements are all zeros. Taking matrix $\mathbf{b}^e_{2,2}$, for example, it can be expressed as

$$\mathbf{b}^e_{2,2} = \begin{bmatrix} \overbrace{0,0,0,\ldots,0,0,0}^{j=1,2,3,\ldots,3N_y} & \overbrace{0,0,0,0,-1/a^2,0,\ldots,0,0,0}^{j=3N_y+1,3N_y+2,3N_y+3,\ldots,6N_y} & \overbrace{0,0,0,\ldots,0,0,0}^{j=6N_y+1,6N_y+2,\ldots,3N} \\ 0,0,0,\ldots,0,0,0, & 0,0,0,0,0,-1/a^2,\ldots,0,0,0, & 0,0,0,\ldots,0,0,0 \\ 0,0,0,\ldots,0,0,0, & 0,0,0,-\dfrac{2}{\kappa(1-\nu)a^2},0,0,\ldots,0,0,0, & 0,0,0,\ldots,0,0,0 \end{bmatrix}. \quad (18)$$

The coefficients in $\mathbf{K}^e$ are determined by equations (14a–c).

2.3. COMPATIBILITY CONDITIONS

In order to obtain a complete solution for the entire plate, the element weighting coefficient matrices, the element displacement vectors and the element consistent mass matrices should be assembled into a global system equations for all the nodal points of the plate labelled from 1 to N. Therefore, the compatibility conditions for the conjunction nodes at the interface boundaries of adjacent elements need to be established. This includes the compatibility conditions for both the displacements and the force and moments.

Obviously, the displacement compatibility conditions are automatically satisfied at all the interface conjunction nodes since the same global nodal number is used for each conjunction node. Only the equilibrium conditions for the force and moments are needed to form the compatibility conditions. According to the locations of the conjunction nodes, the compatibility conditions for the free vibration DQ plate elements are given below:

- *For conjunction nodes at interface boundaries of two elements*: As shown in Figure 3(a), the compatibility conditions for the conjunction nodes at the interface boundaries of two elements l_1 and l_2, which are connected in the x direction, can be expressed according to the equilibrium conditions as

$$(Q^{l_1}_x)_{N_x,j} - (Q^{l_2}_x)_{1,j} = 0, \quad (M^{l_1}_x)_{N_x,j} - (M^{l_2}_x)_{1,j} = 0, \quad (M^{l_1}_{xy})_{N_x,j} - (M^{l_2}_{xy})_{1,j} = 0. \quad (19a\text{–}c)$$

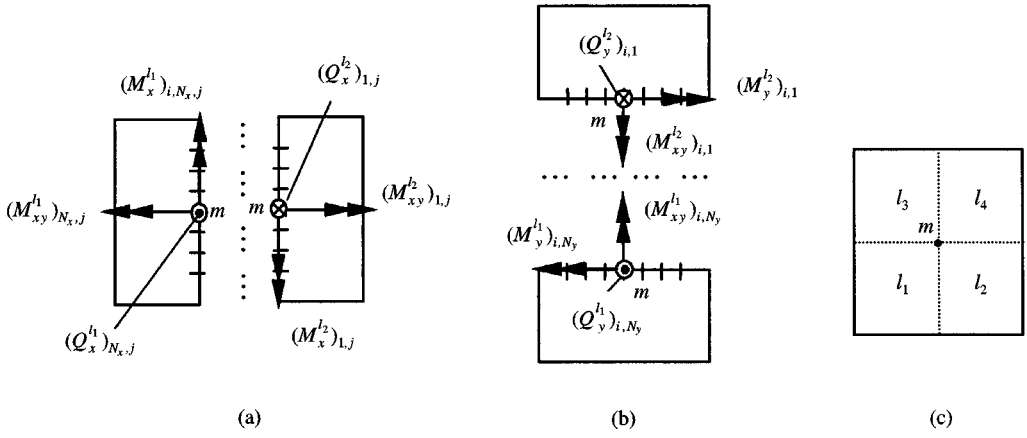

Figure 3. Locations of conjunction nodes on the interface boundaries of adjacent elements: (a) two elements are connected in x direction: (b) two elements are connected in y direction; (c) four elements are connected at node m.

Similarly, for the conjunction nodes at the interface boundaries of two elements l_1 and l_2 connected in the y direction as shown in Figure 3(b), the compatibility conditions are given by

$$(Q_y^{l_1})_{i,N_y} - (Q_y^{l_2})_{i,1} = 0, \quad (M_y^{l_1})_{i,N_y} - (M_y^{l_2})_{i,1} = 0, \quad (M_{xy}^{l_1})_{i,N_y} - (M_{xy}^{l_2})_{i,1} = 0. \tag{20a–c}$$

- *For conjunction nodes at which four elements meet*: If four adjacent elements l_1, l_2, l_3 and l_4 are connected at a node m as shown in Figure 3(c), the compatibility conditions for the common node m are

$$\begin{aligned}
&(Q_x^{l_1})_{N_x,N_y} + (Q_x^{l_2})_{N_x,1} - (Q_x^{l_3})_{1,N_y} - (Q_x^{l_4})_{1,1} = 0,\\
&(M_x^{l_1})_{N_x,N_y} + (M_x^{l_2})_{N_x,1} - (M_x^{l_3})_{1,N_y} - (M_x^{l_4})_{1,1} = 0,\\
&(M_{xy}^{l_1})_{N_x,N_y} + (M_{xy}^{l_2})_{N_x,1} - (M_{xy}^{l_3})_{1,N_y} - (M_{xy}^{l_4})_{1,1} = 0
\end{aligned} \tag{21a–c}$$

or

$$\begin{aligned}
&(Q_y^{l_1})_{N_x,N_y} - (Q_y^{l_2})_{N_x,1} + (Q_y^{l_3})_{1,N_y} - (Q_y^{l_4})_{1,1} = 0,\\
&(M_y^{l_1})_{N_x,N_y} - (M_y^{l_2})_{N_x,1} + (M_y^{l_3})_{1,N_y} - (M_y^{l_4})_{1,1} = 0,\\
&(M_{xy}^{l_1})_{N_x,N_y} - (M_{xy}^{l_2})_{N_x,1} + (M_{xy}^{l_3})_{1,N_y} - (M_{xy}^{l_4})_{1,1} = 0
\end{aligned} \tag{22a–c}$$

The final global matrix forms of equation system for free vibration of the entire plate become

$$\mathbf{Kd} = \lambda \mathbf{Bb}, \tag{23}$$

where **K**, **d** and **B** are the overall weighting coefficient matrix, global displacement vector, and overall mass matrix of the plate.

Solving the final algebraic eigenvalue equation system by the ordinary eigenvalue equation system solver, the solutions to the entire plate can be obtained.

3. NUMERICAL RESULTS AND DISCUSSIONS

Using the method described above, the vibration frequencies of rectangular plates with any arbitrary combination of mixed boundary constraints can be determined easily. In the present study, however, we only focus on six cases as shown in Figure 4(a–f). The grid points employed in computation are designed by

$$x_i = \frac{a}{2}\{1 - \cos[(i-1)\pi/(N_x - 1)]\}, \quad i = 1, 2, 3, \ldots, N_x, \tag{24}$$

$$y_j = \frac{b}{2}\{1 - \cos[(j-1)\pi/(N_y - 1)]\}, \quad j = 1, 2, 3, \ldots, N_y \tag{25}$$

The Poisson's ratio is taken to be $\nu = 0{\cdot}3$. The eigenvalues are expressed in terms of the frequency parameter as $\lambda = \omega a^2\sqrt{\rho h/D}$.

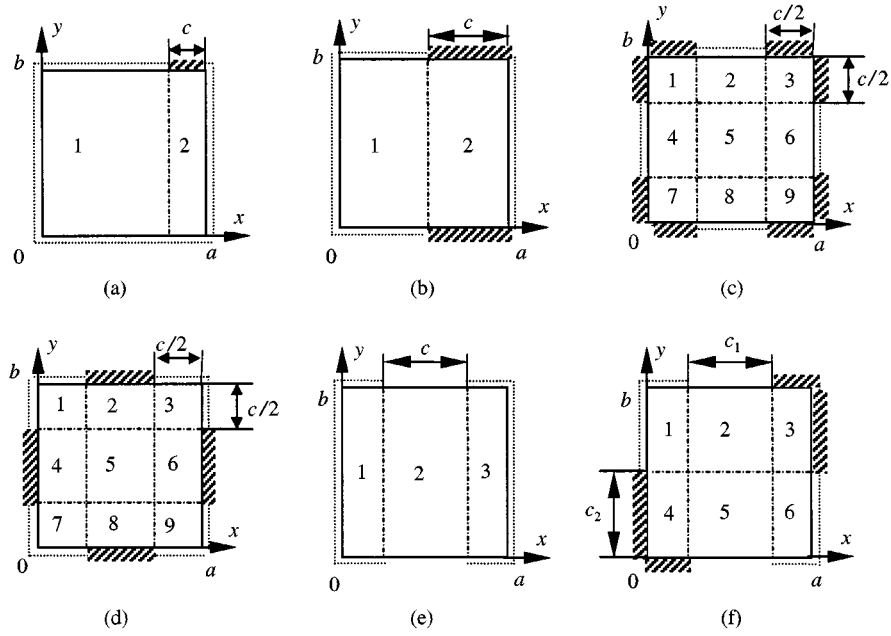

Figure 4. Configurations of rectangular plates with mixed boundary constraints analyzed by present numerical method: (a) a simply supported rectangular plate partially clamped along one edge, (b) a simply supported rectangular plate partially clamped along two opposite edges; (c) a simply supported rectangular plate partially clamped along four edges symmetrically from the corners; (d) a square plate with central portions of edges clampped and the portions around four corners simply supported; (e) a simply supported rectangular plate with central portions of two opposite edges free; (f) a rectangular plate having simply supported, free and clamped constraint conditions at the same edges.

Convergence studies are carried for the example problems (cases a–f) to establish the grid points required in each element for obtaining the accurate solutions. The convergence patterns of the frequency parameters with the number of grid points in each element are presented in Table 1 for cases a–d and in Table 2 for cases e–f.

It can be observed from Tables 1 and 2 that the convergence rate varies for different plate configurations. Generally, the convergence rate of the plate which includes more singular points on boundaries is lower than that of a plate having a lesser number of singular points on the boundaries. And the convergence of frequency parameters for plates having partially free boundary conditions on the mixed boundaries (cases e and f) is slower than that for plates without free boundary conditions on the periphery boundaries. However, for all the cases considered in this paper, a convergence to at least three significant figures can be achieved when 13×13 grid points are used in each element. Therefore, 13×13 grid points in each element will be used to generate all the results in the following studies to ensure the high accuracy of the numerical solutions.

To examine the validity of the numerical method employed, the computed frequency parameters have been compared with the existing solutions available in the open literature. In Table 3, a comparison of the present solutions with those from various sources for cases a–d is presented. Since no solutions have been found for thick plates of cases a–d in the open publications, only the results for the thin plates ($h/a = 0{\cdot}01$) are compared here with the existing thin plate theory solutions. It is evident from Table 3 that the present solutions for the thin plates ($h/a = 0{\cdot}01$) agree very well with the analytical solutions established by Ota and Hamada [1], Keer and Stahl [2], Narita [3] and Gorman [5], and the Rayleigh–Ritz solutions given by Liew *et al.* [9]. However, the results obtained by the finite element method [4], spline finite strip method [6] and the spline element method [7] seem to be slightly higher than those given by the present method and the analytical method. Even so, they are well within the range of the acceptable accuracy for engineering applications.

Based on the convergence and comparison studies, the present numerical solution approach has been employed to determine the vibration frequencies of the thick rectangular plates having various mixed boundary constraints. The frequency parameters corresponding to the first eight modes of free vibration for cases a–f have been computed and presented in Tables 4–9 for rectangular plates of various relative thickness ratios (h/a) and mixed edge constraint ratio (c/a). Some of the results, where possible, are compared with the existing solutions in the literature. For all the cases considered, the dependence of the frequency parameters on both relative thickness ratio and the mixed edge constraint ratio is observed.

In Tables 4 and 5, it is observed that as the partially clamped ratio, c/a, approaches the value 1·0, the frequency parameters approach the values of a square plate with one or two edges fully clamped and the other edges simply supported for all the relative thickness varying from $h/a = 0{\cdot}01$ to 0·2. Also, it is observed that regardless of the relative thickness, the frequency parameters vary only slightly when the partial clamped ratio is within $c/a = 0{\cdot}0$–$0{\cdot}2$ or $c/a = 0{\cdot}8$–$1{\cdot}0$. The significant variations occur, however, in the mid-range of c/a. This phenomenon has been discussed earlier by other researchers for thin plate problems [5, 9]. The

TABLE 1

Convergence of frequency parameters $\lambda = \omega a^2 \sqrt{\rho h/D}$ *with increasing number of the grid points in each element for a square plate* ($h/a = 0{\cdot}1$) *with mixed boundary constraints* (*cases a–d*)

		Mode sequence number							
Case	$N_x \times N_y$	1	2	3	4	5	6	7	8
a	5×5	20·5800	45·5777	84·1521	88·3709	104·048	127·932	162·738	167·750
$c/a = 0{\cdot}5$	6×6	21·0060	45·3880	48·9165	71·1195	84·2639	106·086	130·772	149·536
	7×7	21·1124	45·6841	49·5431	71·6598	85·6318	88·1667	107·242	109·545
	8×8	21·1509	45·7395	49·6484	71·7344	85·4580	90·1179	107·596	110·893
	9×9	21·1656	45·7404	49·6606	71·7528	85·3949	89·4480	107·509	110·194
	10×10	21·1747	45·7425	49·6500	71·7347	85·4044	89·3573	107·501	110·185
	11×11	21·1798	45·7451	49·6602	71·7345	85·4061	89·2280	107·489	110·095
	12×12	21·1833	45·7475	49·6662	71·7351	85·4075	89·2487	107·491	110·099
	13×13	21·1857	45·7485	49·6706	71·7359	85·4076	89·2612	107·494	110·103
b	5×5	22·6575	46·7026	84·6325	90·8073	111·828	132·023	160·864	167·212
$c/a = 0{\cdot}5$	6×6	23·1927	47·1896	51·3033	74·3694	84·7122	107·488	130·991	150·397
	7×7	23·4377	47·2852	52·3448	75·4754	86·0588	91·0545	109·631	114·071
	8×8	23·5041	47·2862	52·3253	74·8898	85·8996	93·5035	109·394	116·698
	9×9	23·5483	47·2919	52·3648	74·9160	85·8458	92·3568	109·377	113·956
	10×10	23·5652	47·2925	52·3859	74·9229	85·8532	92·3010	109·403	114·062
	11×11	23·5809	47·2933	52·4047	74·9217	85·8566	92·2010	109·409	114·003
	12×12	23·5864	47·2938	52·4249	74·9221	85·8576	92·2261	109·418	114·002
	13×13	23·5941	47·2941	52·4324	74·9222	85·8588	92·2482	109·420	114·003

c	5×5	25·8372	53·2219	53·2242	82·6095	87·4281	95·4539	117·889	117·901
$c/a = 2/3$	6×6	26·1419	54·2464	54·2544	84·1686	88·5577	96·3892	119·263	119·265
	7×7	26·1550	54·2643	54·2647	84·1607	88·8201	96·6394	119·483	119·493
	8×8	26·2383	54·3448	54·3483	84·2144	88·8930	96·7107	119·517	119·518
	9×9	26·2603	54·3727	54·3731	84·2276	88·9328	96·7293	119·529	119·533
	10×10	26·2898	54·4062	54·4080	84·2552	88·9705	96·7612	119·555	119·556
	11×11	26·3034	54·4235	54·4238	84·2669	88·9916	96·7789	119·566	119·568
	12×12	26·3181	54·4401	54·4412	84·2801	89·0112	96·7939	119·579	119·579
	13×13	26·3262	54·4505	54·4506	84·2878	89·0229	96·8046	119·585	119·586
d	5×5	30·4226	56·3835	56·7672	76·9366	92·8638	99·8602	111·512	114·401
$c/d = 2/3$	6×6	31·4046	58·8278	60·2112	81·4011	96·9614	101·994	115·053	119·639
	7×7	31·4080	58·8566	60·1536	81·3033	97·2763	102·192	115·137	119·743
	8×8	31·4232	58·8686	60·1833	81·4113	97·2752	102·188	115·259	119·761
	9×9	31·4316	58·8982	60·1776	81·3984	97·3242	102·179	115·247	119·754
	10×10	31·4344	58·9043	60·1934	81·4393	97·3314	102·181	115·297	119·762
	11×11	31·4415	58·9231	60·1929	81·4386	97·3591	102·182	115·298	119·763
	12×12	31·4422	58·9253	60·2002	81·4580	97·3626	102·181	115·323	119·766
	13×13	31·4467	58·9366	60·2002	81·4582	97·3785	102·182	115·324	119·767

TABLE 2

Convergence of frequency parameters $\lambda = \omega a^2 \sqrt{\rho h/D}$ *with increasing number of the grid points in each element for a square plate* $(h/a = 0{\cdot}1)$ *with mixed boundary constraints (case e–f)*

		Mode sequence number							
Case	$N_x \times N_y$	1	2	3	4	5	6	7	8
e	5×5	18·4158	44·1013	47·9030	67·8778	85·0881	87·8688	115·078	128·096
$c/a = 1/3$	6×6	18·5178	41·2398	44·9147	67·3257	68·9756	84·0989	85·9829	108·974
	7×7	18·5968	41·9654	41·0195	68·2262	69·4348	84·6037	87·1892	102·019
	8×8	18·6158	41·9991	45·0243	68·5624	70·9247	84·8291	90·7161	104·539
	9×9	18·6434	42·1940	45·0650	68·5857	70·3221	84·8092	91·7146	104·493
	10×10	18·6516	42·2627	45·0664	68·6293	70·8356	84·8010	91·1472	104·440
	11×11	18·6698	42·3701	45·0834	68·6471	71·1729	84·7951	91·6705	104·456
	12×12	18·6717	42·4129	45·0827	68·6686	71·4087	84·8000	92·0078	104·487
	13×13	18·6842	42·4675	45·0898	68·6784	71·5995	84·8023	92·2459	104·531
	14×14	18·6838	42·4753	45·0893	68·6865	71·7070	84·8049	92·4255	104·544
f	5×5	24·2577	43·7685	55·1378	68·4028	73·6311	86·3611	95·2704	106·535
$c_1/a = 1/3$	6×6	24·4809	44·4021	55·8870	71·4835	75·6167	91·3024	96·1577	108·120
$c_2/b = 0{\cdot}5$	7×7	24·5330	44·6073	56·0533	72·2066	75·9186	93·6428	96·4888	109·084
	8×8	24·5784	44·6854	56·1111	72·3105	76·2283	94·1678	96·4848	109·065
	9×9	24·6297	44·8046	56·1733	72·5153	76·4404	94·6111	95·5001	109·078
	10×10	24·6422	44·8403	56·2144	72·6076	76·6240	94·9493	96·5249	109·142
	11×11	24·6742	44·9041	56·2483	72·6947	76·7552	95·2008	96·5392	109·173
	12×12	24·6780	44·9211	56·2698	72·7407	76·8524	95·3759	96·5513	109·203
	13×13	24·6981	44·9596	56·2903	72·7866	76·9360	95·5246	96·5603	109·220
	14×14	24·6994	44·9682	56·3029	72·8124	76·9437	95·6282	96·5674	109·239

TABLE 3

Comparison studies for frequency parameters $\lambda = \omega a^2 \sqrt{\rho h/D}$ *of a sqaure plate with various mixed boundary constraints* ($h/a = 0{\cdot}01$, $c/a = 0{\cdot}5$)

Case	Sources	Mode sequence number					
		1	2	3	4	5	6
a	Present	22·42	49·84	55·48	82·13	99·47	106·53
	Ota and Hamada [1]	22·4	—	—	—	—	—
	Keer and Stah [2]	22·49	—	—	—	—	—
	Narita [3]	22·63	50·04	55·95	82·34	99·71	
	Gorman [5]	22·48	—	—	—	—	—
	Fan and Cheung [6]	22·73	50·15	56·23	82·98	99·74	—
	Mizusawa and Leonard [7]	22·71	50·10	56·13	82·37	99·73	—
	Liew *et al.* [9]	22·51	49·95	55·72	82·29	99·69	107·1
	Laura and Gutierrez [11]	21·99	—	—	—	—	—
b	Present	25·59	52·04	59·75	87·95	104·34	111·71
	Ota and Hamada [1]	25·5	—	—	—	—	—
	Fan and Cheung [6]	26·37	52·23	61·78	—	—	—
	Liew *et al.* [9]	25·71	52·11	60·09	88·13	110·6	112·3
	Laura and Gutierrez [11]	25·41	—	—	—	—	—
	Striz *et al.* [20]	26·02	52·13	60·80	88·13	100·6	—
c	Present	25·31	57·46	57·46	96·67	100·88	112·88
	Narita [3]	26·18	58·70	58·70	98·58	102·0	—
	Liew *et al.* [9]	25·40	57·63	57·63	97·05	101·1	113·3
d	Present	35·66	71·99	72·04	102·28	125·30	131·01
	Ota and Hamada [1]	35·5	—	—	—	—	—
	Liew *et al.* [9]	35·60	71·71	71·71	101·8	124·8	131·4

frequency parameters decrease as the relative thickness increases, especially pronounced for the higher modes.

The numerical results shown in Tables 6 and 7 are the frequency parameters for square plates with partial portions simply supported and other portions clamped along four edges (cases c and d). In Table 6, it is evident that the frequency parameters for case *c* increase gradually as the clamping ratio c/a increases from $c/a = 0{\cdot}0$ to $1{\cdot}0$. However, it is evident from Table 7 that there are abrupt changes in the frequency parameters at the onset of the partially clamped conditions [$c/a = 0{\cdot}8$–$1{\cdot}0$ as shown in Figure 4(d)]. When the ratio c/a approaches the value $0{\cdot}0$, the frequency parameters approach those of a fully clamped plate in a more gradual manner. This indicated that the effects of the presence of the partially clamped constraint conditions at the middle portions of the plate edges on the frequency parameters are more significant than those at the four corners.

Tables 8 and 9 show the frequency parameters for the last two cases (cases e and f) in which the partial portions of plate edges are free. It is concluded from the results in both tables that all the first eight frequency parameters decrease as the lengths of the free edge portions increase. This indicates that the presence of the free boundary conditions reduces the flexural stiffness of the plate.

TABLE 4

Frequency parameters $\lambda = \omega a^2 \sqrt{\rho h/D}$ *for a simply supported square plate partially clamped along one edge (case a)*

		Mode sequence number							
h/a	*c/a*	1	2	3	4	5	6	7	8
0·01	0·0	19·7319	49·3027	49·3027	78·8410	98·5150	98·5150	127·9993	127·9993
	Dawe [30]	19·7313	49·3026	49·3026	78·8404	98·5144	98·5144	—	—
Exact	Leissa [31]	19·7392	49·3480	49·3480	78·9568	98·6960	98·6960	128·3049	128·3049
	0·2	20·2695	49·3054	50·8555	80·5396	98·5366	100·0949	128·0255	132·3153
	Liew *et al.* [9]	20·33	49·35	51·06	80·80	98·72	100·4	128·3	132·9
	0·4	21·6637	49·4732	53·9809	82·0791	99·1288	103·8443	129·1305	135·3576
	Liew *et al.* [9]	21·77	49·55	54·23	82·22	99·37	104·4	129·6	135·8
	0·6	23·0250	50·4404	56·8170	82·7062	99·5498	109·1678	130·4806	136·3339
	Liew *et al.* [9]	23·10	50·57	57·04	82·98	99·74	109·7	130·9	136·9
	0·8	23·5810	51·4673	58·3949	85·4168	99·8599	112·5682	132·4767	139·3844
	Liew *et al.* [9]	23·60	51·55	58·51	85·67	100·1	112·9	133·0	140·0
	1·0	23·6324	51·6188	58·5652	85·9723	100·0753	112·9437	133·4269	140·4192
	Liew *et al.* [9]	23·65	51·67	58·65	86·13	100·3	113·2	133·8	140·9
0·1	0·0	19·0584	45·4478	45·4478	69·7167	84·9264	84·9264	106·5154	106·5154
	0·2	19·4079	45·4490	46·3395	70·5967	84·9340	85·6756	106·5239	108·3563
	0·4	20·5324	45·5359	48·5688	71·7044	85·2060	87·7422	106·9654	110·0657
	0·6	21·7427	46·1352	50·6572	71·9763	85·4666	90·7912	107·6530	110·4567
	0·8	22·3092	46·9120	51·9118	73·5516	85·6124	92·7783	108·5066	111·9052
	1·0	22·3758	47·0627	52·0899	74·0042	85·7589	93·0642	109·0722	112·5269
0·2	0·0	17·4291	38·0732	38·0732	55·0024	64·9512	64·9512	78·4340	78·4340
	Liew *et al.* [32]	17·4485	38·1519	38·1519	55·1504	65·1453	65·1453	—	—
	0·2	17·6346	38·0737	38·4883	55·3488	64·9542	65·2163	78·4371	78·9999
	0·4	18·3584	38·1135	39·5858	55·8043	65·0503	65·9280	78·5757	79·4593
	0·6	19·1945	38·3941	40·6165	55·9031	65·1385	66·9742	78·7579	79·5936
	0·8	19·6179	38·7820	41·2401	56·4923	65·1954	67·6087	79·0455	79·9985
	1·0	19·6708	38·8602	41·3344	56·6667	65·2477	67·6994	79·2098	80·1603

TABLE 5

Frequency parameters $\lambda = \omega a^2 \sqrt{\rho h/D}$ *for a simply supported square plate partially clamped along two opposite edges* (*case b*)

		Mode sequence number							
h/a	*c/a*	1	2	3	4	5	6	7	8
0·01	0·0	19·7319	49·3027	49·3027	78·8410	98·5150	98·5150	127·9993	127·9993
	Dawe [30]	19·7313	49·3026	49·3026	78·8404	98·5144	98·5144	—	—
Exact	Leissa [31]	19·7392	49·3480	49·3480	78·9568	98·6960	98·6960	128·3049	128·3049
	0·2	20·8153	50·7042	50·9993	82·5448	98·5570	101·3438	131·2991	133·4482
	0·4	23·7890	52·0058	56·0268	87·6068	99·7512	106·6384	132·4741	143·2852
	0·6	27·1923	52·4360	63·8521	88·3232	100·4066	118·2948	135·6685	144·8855
	0·8	28·7760	54·2772	68·7513	93·0406	101·4485	127·7640	137·8256	151·4705
	1·0	28·9216	54·6658	69·1927	94·3594	101·9944	128·6742	139·7646	154·1989
0·1	0·0	19·0584	45·4478	45·4478	69·7167	84·92637	84·9264	106·5154	106·5154
	0·2	19·7602	46·2447	46·4315	71·5730	84·9412	86·3209	107·9395	108·8049
	0·4	22·1091	47·2625	49·8941	74·6567	85·4885	89·4921	108·4811	113·3701
	0·6	24·9652	47·4769	55·1860	75·0799	85·9314	95·7037	110·0295	114·0861
	0·8	26·4648	48·7020	58·7002	77·7063	86·3694	100·5394	110·8247	117·1715
	1·0	32·4894	61·9371	61·9371	86·7780	102·2068	103·1853	123·5955	123·5955
0·2	0·0	17·4291	38·0732	38·0732	55·0024	64·9512	64·9512	78·4340	78·4340
	Liew *et al.* [32]	17·4485	38·1520	38·1519	55·1504	65·1453	65·1453	—	—
	0·2	17·8409	38·4388	38·5372	55·7153	64·9570	65·4597	78·8709	79·1373
	0·4	19·3258	38·9257	40·2660	56·8080	65·1498	66·6853	79·0287	80·2810
	0·6	21·1744	39·0203	42·7422	56·9672	65·3105	68·7717	79·4802	80·4405
	0·8	22·1808	39·5854	44·2736	58·0066	65·4525	70·1092	79·7244	81·4712
	1·0	22·3085	39·7559	44·4669	58·3574	65·5675	70·2846	80·0060	81·8396

TABLE 6

Frequency parameters $\lambda = \omega a^2 \sqrt{\rho h/D}$ *for a simply supported square plate partially clamped along four edges symmetrically from the corners (case c)*

		Mode sequence number							
h/a	*c/a*	1	2	3	4	5	6	7	8
0·01	0·0	19·7319	49·3027	49·3027	78·8410	98·5150	98·5150	127·9993	127·9993
	Dawe [30]	19·7313	49·3026	49·3026	78·8404	98·5144	98·5144	—	—
Exact	Leissa [31]	19·7392	49·3480	49·3480	78·9568	98·6960	98·6960	128·3049	128·3049
	0·2	20·5706	50·6148	50·6149	82·0756	98·5270	101·2944	132·1607	132·1632
	Liew *et al.* [9]	20·60	50·68	50·68	82·24	98·71	101·5	132·6	132·6
	0·4	23·2656	54·5653	54·5657	91·1024	99·2415	108·4295	141·8685	141·8833
	Liew *et al.* [9]	23·33	54·70	54·70	91·42	99·46	108·8	142·4	142·4
	0·6	27·7453	60·9077	60·9078	101·7207	104·2679	117·6520	152·3085	152·3176
	Liew *et al.* [9]	27·87	61·15	61·15	102·2	104·7	118·2	153·1	153·1
	0·8	33·0430	68·7602	68·7604	107·2746	118·2646	127·2459	160·4759	160·4766
	Liew *et al.* [9]	33·23	69·14	69·14	107·7	119·2	128·0	161·3	161·3
	1·0	35·9375	73·2324	73·2324	107·8890	131·1188	131·7522	164·2996	164·2996
	Liew *et al.* [9]	35·99	73·40	73·40	108·2	131·6	132·2	165·0	165·0
0·1	0·0	19·0584	45·4478	45·4478	69·7167	84·9264	84·9264	106·5154	106·5154
	0·2	19·5858	46·1783	46·1783	71·3255	84·9294	86·2389	108·3120	108·3125
	0·4	21·5179	48·6709	48·6712	76·3661	85·1869	90·0820	113·0899	113·0935
	0·6	24·9088	52·7616	52·7617	82·6074	87·3476	95·0594	118·1746	118·1782
	0·8	29·2339	57·9557	57·9561	86·2698	94·0125	100·0377	121·7305	121·7308
	1·0	32·4894	61·9371	61·9371	86·7780	102·2068	103·1853	123·5955	123·5955
0·2	0·0	17·4291	38·0732	38·0732	55·0024	64·9512	64·9512	78·4340	78·4340
	Liew *et al.* [32]	17·4485	38·1519	38·1519	55·1504	65·1453	65·1453	—	—
	0·2	17·7866	38·4696	38·4696	55·7461	64·9525	65·5151	79·1265	79·1267
	0·4	19·0892	39·7921	39·7921	57·9598	65·0430	67·0918	80·8421	80·8431
	0·6	21·3628	41·8623	41·8624	60·4728	65·7928	68·9603	82·4034	82·4043
	0·8	24·2775	44·3325	44·3327	61·7785	68·0637	70·5812	83·2685	83·2686
	1·0	26·4534	46·1349	46·1349	61·9297	70·5488	71·5214	83·6969	83·6969

TABLE 7

Frequency parameters $\lambda = \omega a^2 \sqrt{\rho h/D}$ *for a square plate with central portions of edges clamped and the portions around four corners simply supported* (case d)

		Mode sequence number							
h/a	*c/a*	1	2	3	4	5	6	7	8
0·01	0·0	35·9375	73·2324	73·2324	107·8890	131·1188	131·7522	164·2996	164·2996
	0·2	35·9414	73·2321	73·2323	107·8574	131·1247	131·7170	164·1918	164·1929
	0·4	35·8996	73·0169	73·0375	106·9872	130·7174	131·1311	162·0256	162·4860
	0·6	35·5013	71·4384	71·9516	102·8593	126·0229	131·0986	153·3462	157·8889
	0·8	32·7372	64·3999	64·9865	90·5992	111·4985	125·5724	138·7304	146·5304
	1·0	19·7319	49·3027	49·3027	78·8410	98·5150	98·5150	127·9993	127·9993
0·1	0·0	32·4894	61·9371	61·9371	86·7780	102·2068	103·1853	123·5955	123·5955
	0·2	32·4752	61·8734	61·8852	86·5593	102·2056	102·9603	123·1601	123·2376
	0·4	32·3632	61·4967	61·5624	85·4789	101·8436	102·2495	121·3052	121·8769
	0·6	31·8048	59·8738	60·5993	82·5614	98·7472	102·2254	116·828	120·0274
	0·8	30·3556	56·3506	59·4845	79·5927	94·2211	101·9477	112·9509	119·6739
	1·0	19·0584	45·4478	45·4478	69·7167	84·9264	84·9264	106·5154	106·5154
0·2	0·0	26·4534	46·1349	46·1349	61·9297	70·5488	71·5214	83·6969	83·6969
	0·2	26·4282	46·0828	46·0877	61·8111	70·5494	71·4174	83·5593	83·5705
	0·4	26·2504	45·7579	45·7782	61·138	70·5434	70·8201	82·8252	82·9082
	0·6	25·7163	44·8150	45·1897	59·8430	69·6038	70·5839	81·4740	82·2933
	0·8	24·6335	43·0716	44·6425	58·7117	68·0744	70·5226	80·3515	82·2045
	1·0	17·4291	38·0732	38·0732	55·0024	64·9512	64·9512	78·4340	78·4340

TABLE 8

Frequency parameters $\lambda = \omega a^2 \sqrt{\rho h/D}$ *for a simply supported square plate partially free along central portion of two opposite edges* (*case e*)

		Mode sequence number							
h/a	*c/a*	1	2	3	4	5	6	7	8
0·01	0·2	19·7032	49·0887	49·2266	78·6660	97·3726	98·5017	127·0872	127·7119
	0·4	19·3223	46·2526	49·1094	78·1793	82·2857	98·4244	109·3464	126·1870
	0·6	17·9489	37·4079	48·4752	57·5104	74·9452	84·5854	98·0630	114·0658
	0·8	15·3086	27·4287	44·5607	46·2229	65·0414	78·1043	90·3212	96·2321
0·1	0·2	18·9688	44·7273	45·2506	69·2345	81·7609	84·8962	104·5299	105·8487
	0·4	18·3806	40·1943	44·9621	63·7399	68·0927	83·0393	84·7051	102·7395
	0·6	16·7269	31·0930	44·0991	46·5858	63·7171	70·4994	84·1098	89·1438
	0·8	13·9729	22·9320	38·3113	41·6353	54·1729	67·5186	72·3184	82·0657
0·2	0·2	17·2669	36·9662	37·8752	54·5730	60·9513	64·9314	75·7469	77·8970
	0·4	16·5009	31·8639	37·5109	46·1791	53·2956	59·8742	64·7677	74·7803
	0·6	14·7502	24·4214	35·9174	36·5996	49·1241	54·3304	64·1567	64·2071
	0·8	12·2333	18·5469	31·1711	34·4099	41·8988	52·9609	53·9970	62·4719

TABLE 9

Frequency parameters $\lambda = \omega a^2 \sqrt{\rho h/D}$ *for a square plate having simply supported, free and clamped constraint conditions at the same edges* (*case f*, $c_2/b = 0{\cdot}5$)

		Mode sequence number							
h/a	c_1/a	1	2	3	4	5	6	7	8
0·01	0·2	28·5202	53·1143	68·9142	86·4119	111·2899	122·0728	133·7538	148·1331
	0·4	26·7086	49·5960	65·3659	84·7196	90·8904	116·0664	120·7714	134·5360
	0·6	24·1897	39·6816	60·8285	61·1666	81·9392	88·3379	117·2949	121·9796
	0·8	20·8682	28·9284	47·2733	57·0899	70·2250	80·9607	96·3591	110·9087
0·1	0·2	25·7218	47·2261	58·2256	74·5374	88·6812	97·0398	108·7663	114·9896
	0·4	24·0569	42·7166	55·0997	66·3203	73·8776	85·6998	96·1425	107·2972
	0·6	21·5997	32·8643	48·1098	52·2427	68·3299	72·5401	92·7412	93·8581
	0·8	18·6420	24·5777	39·8452	49·0395	58·0647	68·9074	75·4648	89·9096
0·2	0·2	21·7196	38·3171	44·0336	57·2673	63·0577	68·9444	77·4884	80·6879
	0·4	20·2634	33·2580	42·1687	46·9952	55·9363	61·0501	68·5758	76·5097
	0·6	18·0982	25·5000	36·5300	40·6084	51·2475	55·1585	65·3044	67·5281
	0·8	15·7477	19·9065	31·9287	38·2642	43·9951	53·3836	55·3314	65·4473

The variation trends of the frequency parameters with the relative thickness ratio h/a shown in Tables 6–9 are all very similar to those for cases a and b observed in Tables 4 and 5, i.e. the frequency parameters decrease as the relative thickness ratio increases.

4. CONCLUSION

This paper considers the free vibration of moderately thick rectangular plates with mixed boundary constraints. A new numerical method, the differential quadrature element method, was used to perform the analysis. By using this method, the discontinuities of the boundary constraints are isolated by decomposing the whole solution domain into several continuous sub-domains and the accurate solutions are obtained. The convergence and comparison studies were carried out to establish the reliability and accuracy of the numerical results. Several example rectangular plates with various mixed constraint conditions have been analyzed and the numerical results for the first eight frequency parameters were presented consequently. The effects of the ratio of mixed constraints portion on plate boundaries and those of the plate relative thickness on the frequency parameters of plates have been discussed. Since the solutions for the frequencies of thick plates with various mixed boundary constraints are scarcely reported in the literature, the present solutions should be valuable to engineers and designers for their reference.

REFERENCES

1. T. OTA and M. HAMADA 1963 *Bulletin of Japan Society of Mechanical Engineering* **6**, 397–403. Fundamental frequencies of simply supported but partially clamped square plates.

2. L. M. KEER and B. STAHL 1972 *Journal of Applied Mechanics* **39**, 513–520. Eigenvalue problems of rectangular plates with mixed edge condtions.
3. Y. NARITA 1981 *Journal of Sound and Vibration* **77**, 345–355. Application of a series-type method to vibration of orthtropic rectangular plates with mixed boundary conditions.
4. R. VENKATESWARA, G. RAJU and T. V. MURTHY 1973 *Journal of Sound and Vibration* **30**, 257–260. Vibration of rectangular plate with mixed boundary conditions.
5. D. J. GORMAN 1984 *Journal of Sound and Vibration* **93**, 235–247. An exact analytical approach to the free vibration analysis of rectangular plates with mixed boundary conditions.
6. S. C. FAN and Y. K. CHEUNG 1984 *Journal of Sound and Vibration* **93**, 81–94. Flexural free vibrations of rectangular plates with complex supported conditions.
7. T. MIZUSAWA and J. W. LEONARD 1990 *Engineering Structures* **12**, 285–290. Vibration and buckling of plates with mixed boundary conditions.
8. K. M. LIEW, K. C. HUNG and K. Y. LAM 1993 *Journal of Sound and Vibration* **163**, 451–462. On the use of the substructure method for vibration analysis of rectangular plates with discontinuous boundary conditions.
9. K. M. LIEW, K. C. HUNG and M. K. LIM 1993 *International Journal of Mechanical Science* **35**, 615–632. Roles of domain decomposition method in plate vibrations: treatment of mixed discontinuous periphery boundaries.
10. K. M. LIEW, K. C. HUNG and M. K. LIM 1994 *Journal of Sound and Vibration* **178**, 243–264. On the use of the domain decomposition method for vibration of symmetric laminates having discontinuous at the same edge.
11. P. A. A. LAURA and R. H. GUTIERREZ 1994 *Journal of Sound and Vibration* **173**, 702–706. Analysis of vibrating rectangular plates with non-uniform boundary conditions by using the differential quadrature method.
12. T. SAKIYAMA and H. MATSUDA 1987 *Journal of Sound and Vibration* **113**, 208–214. Free vibration of rectangular Mindlin plate with mixed boundary conditions.
13. R. E. BELLMAN and J. CASTI 1971 *Journal of Mathematical Analysis and Applications* **34**, 235–238. Differential quadrature and long term integration.
14. C. W. BERT, S. K. JANG and A. G. STRIZ 1988 *AIAA Journal* **26**, 612–618. Two new approximate methods for analyzing free vibration of structural components.
15. A. G. STRIZ, S. K. JANG and C. W. BERT 1988 *Thin-Walled Structures* **69**, 51–62. Non-linear bending analysis of thin circular plates by differential quadrature.
16. C. W. BERT, S. K. JANG and A. G. STRIZ 1989 *Computational Mechanics* **5**, 217–226. Non-linear bending analysis of orthotropic rectangular plates by the method of differential quadrature.
17. C. W. BERT and M. MALIK 1996 *Applied Mechanics Review* **49**, 1–28. Differential quadrature method in computational mechanics: a review.
18. A. G. STRIZ, W. CHEN and C. W. BERT 1994 *International Journal of Solids and Structures* **31**, 2807–2818. Static analysis of structures by the quadrature element method (QEM).
19. W. CHEN, A. G. STRIZ and C. W. BERT 1997 *International Journal of Numerical Methods in Engineering* **40**, 1941–1956. A new approach to the differential quadrature method for fourth-order equations.
20. A. G. STRIZ, W. CHEN and C. W. BERT 1997 *Journal of Sound and Vibration* **202**, 689–702. Free vibration of high-accuracy plate elements by the quadrature element method.
21. X. W. WANG and H. Z. GU 1997 *International Journal of Numerical Methods in Engineering* **40**, 759–772. Static analysis of frame structure by the differential quadrature element method.
22. H. Z. GU and X. W. WANG 1997 *Journal of Sound and Vibration* **202**, 452–459. On the free vibration analysis of circular plates with stepped thickness over a concentric region by the quadrature element method.
23. J.-B. HAN and K. M. LIEW 1996 *Proceedings of the 3rd Asian-Pacific Conference on Computational Mechanics*, 2363–2368. The differential quadrature element method (DQEM) for axisymmetric bending of thick circular plates.

24. F.-L. Liu and K. M. Liew 1998 *ASME Journal of Applied Mechanics* **65**, 705–710. Static analysis of Reissner–Mindlin plates by differential quadrature element method.
25. F.-L. Liu and K. M. Liew 1999 *International Journal of Solids and Structures*, **36**, 5101–5123. Differential quadrature element method for static analysis of Reissner–Mindlin polar plates.
26. F.-L. Liu 1999 *International Journal of Solids and Structures*, Rectangular thick plates on Winkler foundation: differential quadrature element solutions (in press).
27. F.-L. Liu and K. M. Liew 1999 *Transactions of ASME*, *Journal of Vibration and Acoustics* **121**, 204–208. Vibration analysis of discontinuous Mindlin plates by differential quadrature element method.
28. F.-L. Liu and K. M. Liew 1999 *Computer Methods in Applied Mechanics and Engineering*, Differential quadrature element method: a new approach for free vibration analysis of polar Mindlin plates having discontinuities (in press).
29. R. D. Mindlin 1951 *ASME Journal of Applied Mechanics* **18**, 31–38. Influence of rotary inertia and shear on flexural motion of isotropic, elastic plates.
30. D. J. Dawe 1985 *Aspects of the Analysis of Plate Structures* 73–99. Oxford: Clarendon Press. Buckling and vibration of plate structures including shear deformation and related effects.
31. A. W. Leissa 1973 *Journal of Sound and Vibration* **31**, 257–293. The free vibration of rectangular plates.
32. K. M. Liew, Y. Xiang and S. Kitipornchai 1994 *Computers and Structures* **49**, 1–29. Transverse vibration of thick rectangular plates — I: comprehensive sets of boundary conditions.